The design of responsible details of an axial piston hydraulic machine improving

The design of responsible details of an axial piston hydraulic machine improving

I V Nikolenko[1], Yu M Khomyak[2], V M. Zheglova[2], O G Kibakov[3] and S O Medvedev[3]

[1]Academy of Construction and Architecture of the Crimean Federal University, Simferopol, Russia
[2]Odessa National Polytechnic University, Odessa, Ukraine
[3]Odessa National Maritime University, Odessa, Ukraine

E-mail energia-09@mail.ru, vheglova@gmail.com

Abstract. Methods of improving the designs of the most complex details of the axial piston hydraulic machine (APHM), cylinder block (CB) and face distributor (FD) are proposed in order to increase their strength. The possibility of modernization is demonstrated by the example of APHM 210.25 with a CB inclined. For samples of CB material, bronze CuSn12, tests were performed and fatigue curves are constructed. Based on the results of these tests, the endurance limit of the CB is determined using the theory of similarity fatigue fracture. The calculation of the BC by the finite element method showed that maximum stresses arise in its inter-cylinder wall (jumper). With conserved CB dimensions, a decrease in the maximum stress level by 30% is achieved if the axial cylinders are shifted in the peripheral direction by 2 ... 3 mm. In the proposed design of the CB the calculated stresses became lower than its endurance limit. For FD an increase in the thickness of its peripheral zone was proposed, which also made it possible to reduce stresses by 12%. As a result, the level of acting stresses turned out to be 5.3% lower than the FD endurance limit. The achieved reduction in stress level for the considered details and an increase in their durability is a factor that growing the environmental safety of APHM.

1. Introduction

The advantages of hydraulic machines (compactness, versatility, ease of operation, energy efficiency, high dynamic characteristics) ensure their widespread use in aviation, land and water transport, housing and communal services, the agricultural complex, etc. [1]. Energy efficient determines continuous expansion of the scope of APHM applications, from mobile military equipment to seawater desalination systems by reverse osmosis for domestic use.

In recent years, much attention has been paid to improving energy efficiency. Many energy saving strategies have been successfully developed and implemented [2, 3]. In particular, the use of a hydraulic drive in a wind power installation increases its efficiency by 17% and raises its efficiency to 90.7% [4]. The use of hydraulic components, such as electric pumps, hydraulic motors, electronic control systems, allows in some industrial systems to reduce energy consumption by 50...70% [5]. The experiments showed that the use of a hydraulic drive in a lifting device with optimal control leads to a reduction in energy consumption by 64% [6].

The development of industrial equipment is associated with an increase in its energy and dynamic characteristics. Improving the APHM is primarily aimed at increasing the working pressure and

IOP Conf. Series: Earth and Environmental Science **408** (2020) 012006 doi:10.1088/1755-1315/408/1/012006

rotation frequency. The requirement of resource saving obliges to ensure minimum weight and dimensions. As a result, during the operation of APHM, stresses in their parts increase, temperature rises, this leads to an increase in the frequency of failure cases [7, 8]. To clarify the causes of failures, methods for analyzing the kinematics and dynamics of APHM [9–12] are developed and refined, and mathematical modeling is improved [13–15]. The accuracy of calculations is achieved using the finite element method (FEM) in a three-dimensional setting [16–18]. Calculation results are checked during field tests [19]. The increase in pressure causes a growth in the forces of contact interaction and the intensification of wear during of details relative moving. To wear reducing new anti-friction materials are developed, working fluids are improved, and methods for cleaning them are improve [20, 21].

Despite said measures, in many cases it is not possible to achieve the required high level of working pressures and speeds. Therefore, instead of copper alloys, it is proposed to use high-strength steels as a material for the CB [22]. This decision seems unsuccessful, since with steel pistons the friction coefficient in the steel-steel pair will be an order of magnitude greater than, for example, in the tin bronze and steel pair. An increase in friction forces leads to a decrease in mechanical efficiency, unacceptable overheating of parts and accelerated wear.

In recent decades, technologically more complex composite or precast constructions of increased strength have begun to be used. When choosing materials for various parts, the APHM follow are strive to provide with their required local quality and take into account the technological capabilities of production. If CB is made of steel to ensure strength, then to reduce friction losses for the contact surfaces it is recommended copper alloys surfacing [23]. Another solution to the problem is to reinforce the bronze block outside with a shell made of high-strength steel [24]. Cavities can be created under the shell, into which the working fluid for hydraulic discharging of the CB is fed through special channels.

The most responsible and at the same time the most loaded element of any APHM is the pumping unit. Its main details are pistons with connecting rods, a drive shaft, bearings, a CB and an FD. The methods of designing and calculating these details, except for the last two, are well developed. At the same time, CB and FD account for about 30% of APHM failures [12, 14], a significant part of which are fatigue fractures. Therefore, when calculating their strength and durability, in order to ensure high reliability, one should focus on the characteristics of fatigue resistance.

2. The goals and objectives of the study

The purpose of the work is to improve the responsible details of the pumping unit of the APHM in order to increase their strength without significantly complicating the design.

In the process, the following tasks are solved:

– determination of the characteristics of strength and fatigue resistance of materials of the details in question;

– calculation of the characteristics of the fatigue resistance of the details under study based on the statistical theory of the similarity of Serensen-Kogaev fatigue failure;

– modeling of details for the purpose of their calculation in the ANSYS Workbench software package and analysis of strength using FEM.

Reducing stresses in the CB and FD below the endurance limit will lead to increased reliability and environmental safety of APHM.

All calculations were performed for the nominal pressure of the working liquid q = 25 MPa. Based on the results of strength calculations of the studied structures, options with the lowest level of maximum stresses were selected.

With increasing pressure q, the maximum stresses will proportionally increase due to the linearity of the formulation of the problems under consideration.

3. Improving the cylinder block

As a result of relative movements between the CB, FD and pistons, sliding friction occurs. To reduce wear, copper alloys are used as the material for CB, the best of which are tin bronzes. In this work, the object of study is the seven-piston APHM 210.25 (Fig. 1).

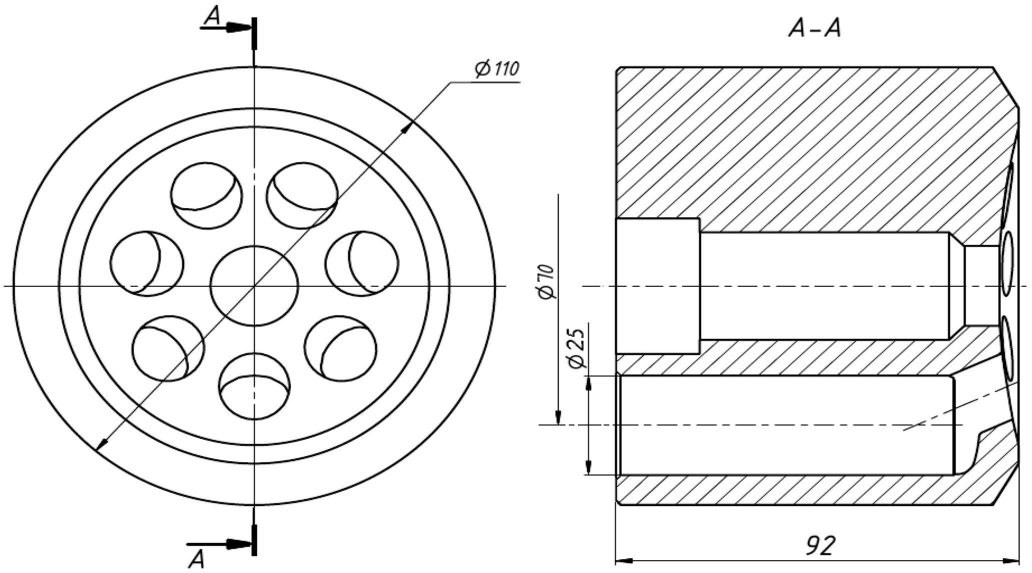

Figure 1. The block of cylinders APHM 210.25.

The most promising material for the CB is bronze CuSn12, which has a low coefficient of friction, high thermal conductivity and wear resistance. Its main components: tin – 12%, lead – 1.3%, nickel – 1%, the rest – copper. This bronze has rather high mechanical characteristics: ultimate strength σ_u=320 MPa, conditional yield strength $\sigma_{0.2}$ =180 MPa, elongation at break δ=12%, hardness 101...104 HB.

Large volumes of loaded axial cavities and instability of pressure lead to the appearance in the CB of complex, cyclically variable stress fields. Such character of loading causes damage accumulation and, in some cases, leads to fatigue failure. In this regard, CB should be calculated for fatigue resistance. For such a calculation, it is necessary to establish the fatigue characteristics of the CB material bronze CuSn12. To this aim tests of its samples were conducted (Fig. 2).

The tests were carried out at a clean circular bend. The sizes of smooth (corset) and notched samples are shown in Table 1. The values of the theoretical stress concentration coefficients *Kt* calculated from the Neuber dependences also here are presented.

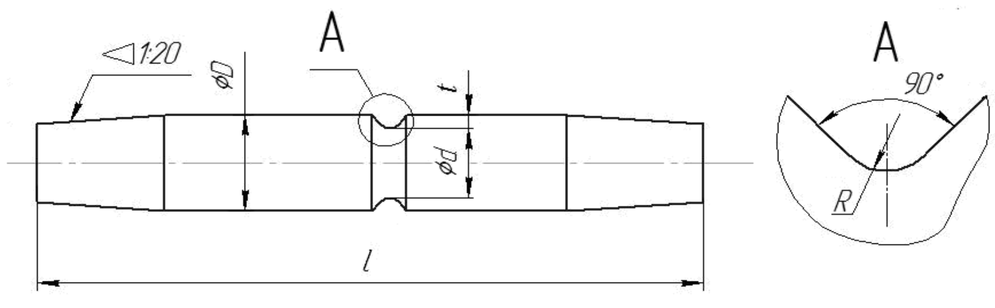

Figure 2. The sample for fatigue test.

Table 1. Characteristics of samples for fatigue tests.

Form of the working part	Sizes, mm					K_t
	l	D	d	t	R	
Smooth	100	11	7.5	1.75	75	1.014
Notched up	100	11	7.5	1.75	1.0	1.737

The equation of the inclined branch of the fatigue curve in power form is presented

$$\sigma^m N = \sigma_{-1}^m N_G = 10^C = \text{const}, \tag{1}$$

where σ and N – the amplitude of the alternating stress and the corresponding number of cycles to failure; m and C – the parameters of equation (1); σ_{-1} – the material endurance limit for a symmetric stress cycle; N_G – the abscissa of the fracture point of the fatigue curve constructed in double logarithmic coordinates.

According to the results of fatigue tests and correlation-regression analysis, the characteristics of equation (1) are calculated and are presented (Table 2 and Fig. 3).

Table 2. Bronze CuSn12. Characteristics of the fatigue curves.

Forms of working surfaces of samples	Designation	m	C	N_G, cycles	σ_{-1}, MPa
Smooth (corset)	•	7.14	21.94	$2.365\cdot10^7$	110
Notched up, Fig. 1	■	7.84	22.56	$1.228\cdot10^8$	70

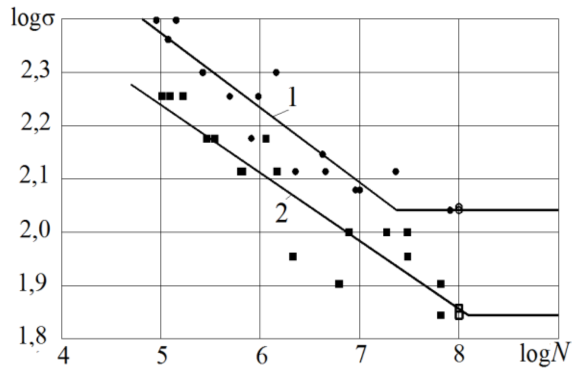

Figure 3. Fatigue curves for tested samples: 1 – smooth; 2 – notched up.

The median value of the endurance limit for a CB is determined using the statistical theory of the similarity of Serensen-Kogaev fatigue fracture [25–27] through the endurance limit of σ_{-1} according to the method of standard GOST 25.504-82

$$\overline{\sigma}_{-1D} = \sigma_{-1} K_V K_A \Big/ [2K_t/(1+\theta^{-\nu_\sigma}) + 1/K_F - 1], \tag{2}$$

where θ – the similarity criterion for fatigue failure; K_A, K_F, K_t, K_V, – respectively are the coefficients of anisotropy, the effect of surface roughness, stress concentration and surface hardening; ν_σ – the coefficient of sensitivity to stress concentration and influence of dimensions of the detail.

Calculations by formula (2) for CB at symmetric cycle of stresses change gave value $\overline{\sigma}_{-1D} = 57.5$ MPa.

In APHM the loading of the cylinders changes according to the pulsating cycle of the alternating stresses. The endurance limit $\overline{\sigma}_{0D}$ with such a cycle was calculated for the CB using the Soderberg formula

$$\sigma_a / \overline{\sigma}_{-1D} + \sigma_m / \sigma_{0.2} = 1, \tag{3}$$

where σ_a and σ_m – the amplitude and mean stresses of the cycle of variable stresses, respectively, $\overline{\sigma}_{-1D}$ – the median value of the endurance limit of the CB with a symmetric cycle; $\sigma_{0.2}$ – conditional yield strength.

With the pulsating cycle of stress variation, the average stresses σ_m are equal to the amplitude σ_a, with σ_a=0,5σ_{max} and $\sigma_{max} = \overline{\sigma}_{0D}$. For these values, according to dependence (3), a formula is obtained for the endurance limit of CB with a pulsating cycle of stress variation

$$\overline{\sigma}_{0D} = \frac{2\overline{\sigma}_{-1D} \cdot \sigma_{0.2}}{\overline{\sigma}_{-1D} + \sigma_{0.2}}. \tag{4}$$

Calculation according to formula (4) gives for CB the value of endurance limit $\overline{\sigma}_{0D} = 87.1$ MPa.

For calculate the stress state the FEM program of the ANSYS Workbench software is used. The number of cylinders in the injection zone varies from three or four and in the discharge zone, respectively, four or three. The calculations were carried out in a three-dimensional setting with a breakdown of the part into finite elements – tetrahedrons with ten nodes. According to the number of axial holes in the discharge zone, three or four, two calculation options were performed at a pressure of q=25 MPa. These calculations were carried out for each analyzed design option.

It was established that the highest stresses occur in the CB with the location of four axial channels in the injection zone. The maximum of the first main stress σ_{1max}=113 MPa takes place in the inter-cylinder partition (ICP), where its thickness is minimal (Fig. 4, *a*). The maximum radial stresses acting normal x to the cross-section of the partition vary in the range (102...104) MPa and are concentrated on a section about 3 mm long. The area of action of radial stresses with a level of (94 ... 104) MPa has a length of about 22 mm (Fig. 4, *b*). In the middle zone of the inter-cylinder partition the voltage is less than in the peripherals by 30 ... 35%. The calculated value of the maximum radial stress σr=104 MPa (Fig. 4, *b*) exceeds the endurance limit $\overline{\sigma}_{0D} = 87.1$ MPa by 19.4%. Therefore, the CB resource is limited and is approximately N=10^7 cycles.

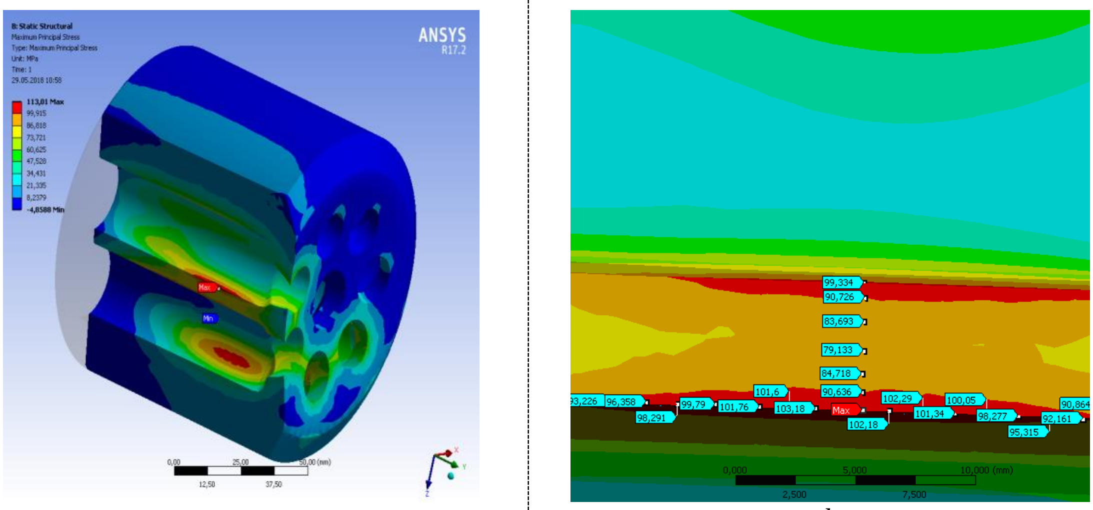

a *b*

Figure 4. The stress state of the BC under the action of pressure q = 25 MPa in four cylinders: *a* – distribution of the principal stresses σ_1 in the longitudinal section of the ICP; *b* – the character of the change in radial stresses along the length and thickness of the danger zone of the ICP.

Analysis shows that the stress state of the serial CB is substantially heterogeneous, since in its outer regions the stresses are much less than the maximum stresses in the ICP (Fig. 4, *a*). To improve the design of the CB, it is proposed to change the location of the axial cylinders so that the stresses are redistributed: decreased in the ICP and increased in the external partitions.

To reduce the stress level in the ICP, a simple design change is proposed, namely, a slight displacement of the axes of the cylinders in the CB diametric planes (Fig. 5). The displacement of the axes of the cylinder holes in the inlet and bottom parts, $\Delta=\Delta_A$ and $\Delta=\Delta_B$, respectively, will be considered positive if they are directed along the radius *r* from the central axis *Oy*. With a positive offset, the thickness of the partitions between the axial holes increases and the thickness of the outer partition decreases. The minimum values of these thicknesses, respectively, t_i and t_e, are determined by the dependences

$$t_i = (D_c + 2\Delta)\sin\frac{\pi}{n} - d_0, \tag{5}$$

$$t_e = 0{,}5(D_e - D_c - 2\Delta - d_0), \tag{6}$$

where D_e=110 mm is the outer diameter of the CB; D_c=70 mm is the diameter of the arrangement of the centers of the axial holes in the serial design; d_0=25 mm — diameters of these holes; n=7 – their number (fig. 5).

The calculation results of the thickness of the partitions according to formulas (5) and (6) at increasing diameter D_c, i.e. at positive displacements, are presented (Fig. 6). Established, that the radial displacement of the piston cavities in the positive direction, but not more than 3.5 mm, is preferable. Negative displacements Δ_B turned out to be irrational, since in this case the maximum stresses in ICP increase.

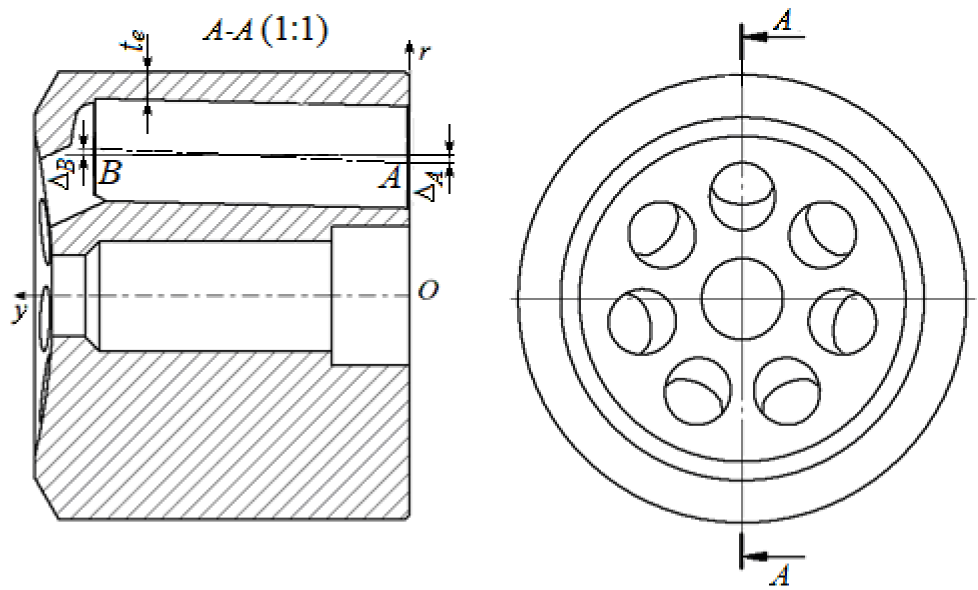

Figure 5. Scheme of CB modernization by displacement of axial cylinder bore axes in diametric planes.

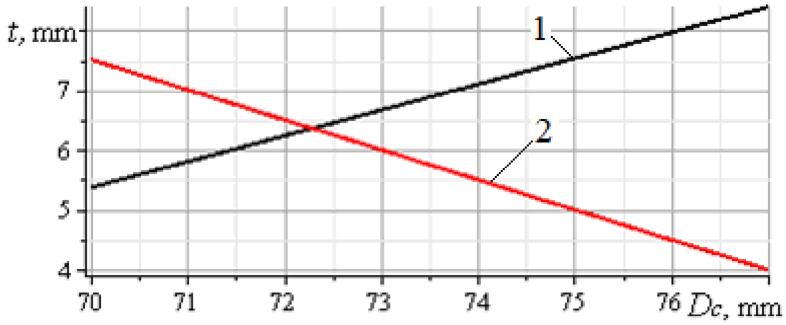

Figure 6. Change in the thickness of the partitions: 1 – inter-cylinder; 2 – external.

As a result of modeling and calculations in the ANSYS Workbench software package, the stresses in the CB of several modernized models were determined. The maximum stresses in the considered models arise in the ICP. Their values are given in Table 3.

Table 3. The maximum stresses in the CB with displacements of the axes of the cylinders.

Δ_A, mm	–1.5			0			+0.5
Δ_B, mm	–1.5	+4	+3	+2	+1	0	–0.5
Von Mises stress, $\sigma_{M\max}$, MPa	165	132	106	110	121	139	214
Principal stress, $\sigma_{1\max}$, MPa	137	109	77	79	93	113	204

The best of the considered upgrade options turned out to be CBs with axial displacements Δ_B=+2...3 mm at Δ_A=0 (Table 3). In these variants, the stresses are reduced in comparison with the initial design with Δ_A=Δ_B=0 by 30% (Fig. 7, 8).

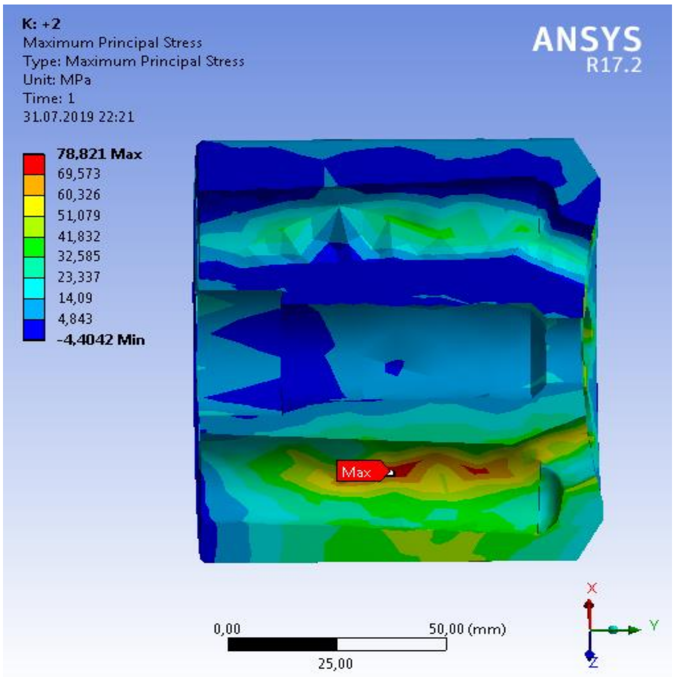

Figure 7. Distribution of the first main voltage in the advanced CB with Δ_A=0 and Δ_B=+2 mm.

In the calculations the number of finite elements and nodes are equal to 400 000...600 000. The calculation time of each option was 3...4 minutes.

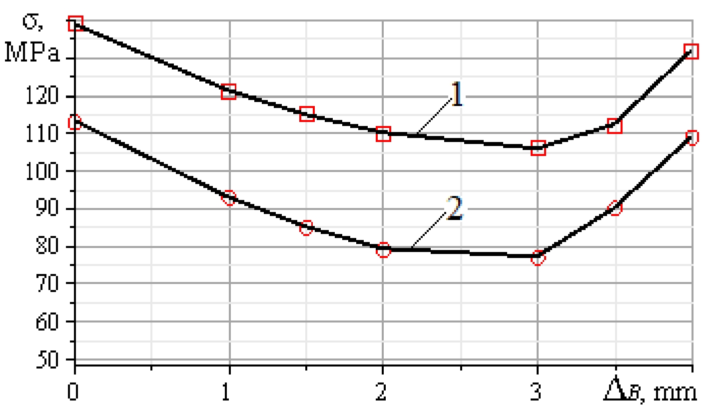

Figure 8. The values of the maximum stresses depending on the displacement Δ_B at $\Delta_A = 0$: 1 – Von Mises stress, σ_{Mmax}; 2 – principal, σ_{1max}.

At displacements Δ_B>3 mm, stresses increase both in ICP and in the external partitions of the CB.

The second upgrade option is to change the shape of the transition surface from the cylinder cavities to the exhaust channels in the front of the CB. It is proposed to replace the flat surface with a conical transition with an apex angle of 120 ° ... 150 ° (Fig. 9).

The calculations showed that when replacing the flat form on the conical transition, the stresses values are practically unchanged, but in this design the conditions for the flow of the working fluid to the distributor are improved and the noise level will be reduced. The conical transition can be combined with the displacement of the axes which was proposed in the first embodiment.

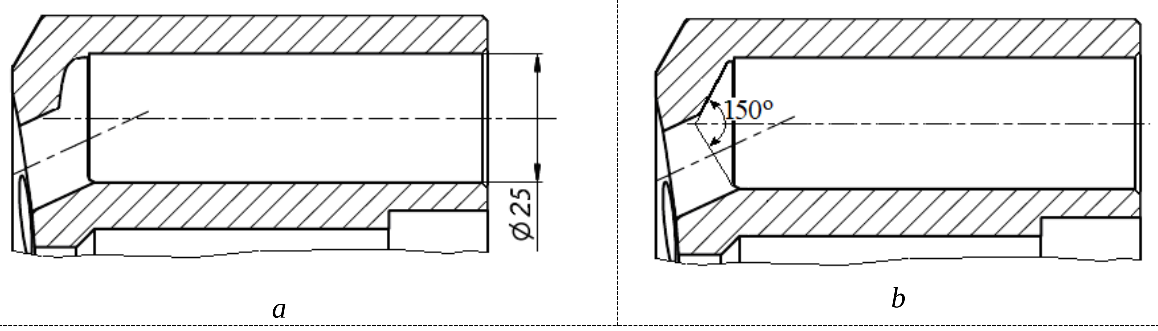

Figure 9. The design of the inner surface of the cylinder cavities in the front of the CB: *a* – serial; *b* – modernized.

4. The FD improvement

APHM 210.25 has FD material – low-alloy chromium-molybdenum steel (its counterpart in the European Union is 41CrAlMo7 steel). The main components of this steel: carbon – 0.35...0.42%, chromium 1.35...1.65%, silicon 0.20...0.45%, manganese 0.15...0.25%, molybdenum 0.15...0.25%, aluminum 0.7...1.1%. Chemical heat treatment is normalization and nitriding of the surface.

The mechanical characteristics of this steel are: conditional yield strength $\sigma_{0.2}$=580...590 MPa, ultimate strength σ_u=760...790 MPa, endurance limit σ_{-1}=420...450 MPa for smooth samples with a diameter of 7.5 mm.

Machining after nitriding – grinding to the arithmetic mean deviation of the profile of the irregularities Ra=1.6 µm.

The main load acting on the FD is the pressure q of the working fluid in the injection window. The nature of loading of serial and modified spherical FDs (Fig. 10).

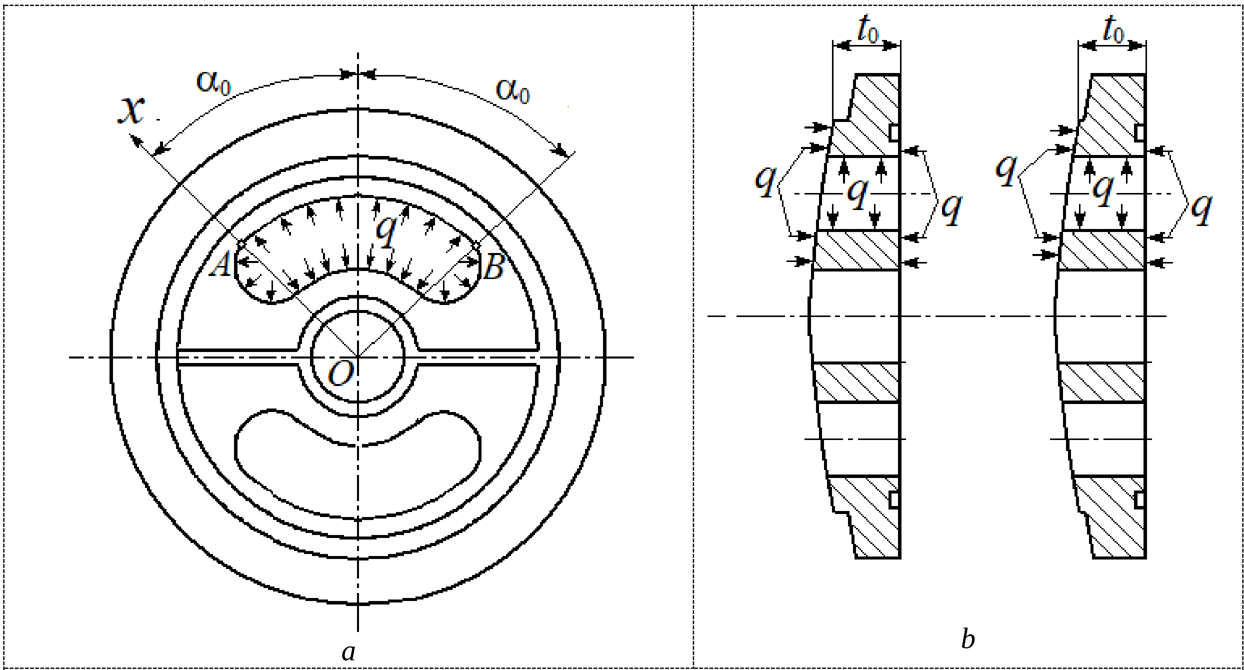

Figure 10. Face distributor: *a* – view from the side of the surface facing the housing cover: *b*, *c* – cross-sectional shape before and after modification.

The stresses arising in the FD under the action of pressure q = 25 MPa are determined using the FEM. Their maximum values arise in the boundary zones of the outer wall of the high-pressure window, in the vicinity of points *A* and *B*. It was found that a rather simple modification of the structure (the thickness of the peripheral zone was increased by 1.5 mm) (fig. 10, *c*), it decreases the value of the maximum principal stress: from σ_{1max}=176 MPa in a serial FD (SFD) to σ_{1max}=157 MPa in a modified (MFD), i.e. by 12% [18]. The stress distribution σ_{1max} in the radial section of the outer wall passing along the line *Ax* is presented in table 4.

Table 4. Distribution of the principal stresses in the dangerous section of the FD.

Coordinate *Ax*, mm		0	1.0	2.5	4.0	5.5
Serial FD	σ_{1S}, MPa	176	140	77	46	21
Modified FD	σ_{1M}, MPa	157	114	79	58.5	40.5

A similar picture is obtained in a symmetrically located neighborhood of point B.

From the analysis given in table 4 values it follows that, along with a decrease in the magnitude of the principal stress of the MFD, the gradient of these stresses $G=d\sigma_1/dx$ in the vicinity of hazardous points *A* and *B* becomes much smaller. The calculations give the following values of the gradients near points *A* and *B*: for the SFD G_S =81.8 MPa/mm, for the MFD G_M=53.0 MPa/mm. With a cyclic change in stresses a decrease in the magnitude of the stress gradient decreases the rate of fatigue failure.

In work [18] the values of endurance limits were determined for pulsating cycle of stress variation, for SFD σ_{0S}=166.2 MPa, for MFD σ_{0M}=165.3 MPa with a 98% probability of distributor non-fracture. It follows from the calculations that the SFD has $\sigma_{0S}< \sigma_{1S}$=176 MPa, i.e. SFD life will be limited. At MFD we have $\sigma_{0M}> \sigma_{1M}$=157 MPa and unlimited durability is ensured.

5. Summary

1. It is shown in the paper that an increase in strength can be achieved without the use of additional reinforcing elements, due to the improvement of the structures of the parts of the pumping unit. Simple methods have been proposed for increasing the constructive strength and cyclic durability of the most complex in form APHM details – the cylinder block and the face distributor.
2. An algorithm for numerically-analytical determination of stress concentration factors has been developed for details of complex configuration, based on the FEM.
3. The possibility of calculating the resource of details with the localization of dangerous stresses in small volumes by the methods of the statistical theory of similarity of fatigue failure is shown.
4. For a serial axial piston hydraulic machine 210.25, if the axial cylinders are offset in the radial direction by 2.5 mm, the maximum stresses are reduced by 30%.

References

[1] Altare G and Vacca A A 2015 Design Solution for Efficient and Compact Electro-hydraulic Actuators *Procedia Engineering* **106** pp 8-16 https://doi.org/10.1016/j.proeng.2015.06.003
[2] Aly A A and Salem F A, Hanafy T S 2014 Energy Saving Strategies of an Efficient ElectroHydraulic Circuit (A review) *International Journal of Control, Automation and Systems* Vol 3 **3** pp 6–10 https://pdfs.semanticscholar.org/d0f4/c1c8b4ce193944567338083909a871ffc9b6.pdf
[3] Karpenko M and Bogdevicius M 2017 Review of Energy-Saving Technologies in Modern Hydraulic Drives *Civil and Transport Engineering, Aviation Technologies* **9(5)** pp 553–558 https://journals.vgtu.lt/index.php/MLA/article/download/427/301
[4] Pusha A, Deldar M and Izadian A 2013 Efficiency Analysis of Hydraulic Wind Power *Transfer System IEEE International Conf. on Electro-Information Technology EIT* Rapid City SD USA p 7 https://ieeexplore.ieee.org/abstract/document/6632717
[5] Rydberg K-E 2015 Energy Efficient Hydraulics – System Solutions for Minimizing Losses *National Conference on Fluid Power Linköping University* Linköping Sweden p 10 https://www.researchgate.net/publication/293333078_Energy_Efficient_Hydraulics_-_System Solutions_for_Minimizing_Losses
[6] Koitto T, Kauranne H, Calonius O, Minav T and Pietola M 2019 Experimental Study on Fast and Energy-Efficient Direct Driven Hydraulic Actuator Unit *Energies* **12** **1538** p 17 https://aaltodoc.aalto.fi/handle/123456789/38230
[7] Avrunin G A, Pimonov I G and Moroz I I 2015 Practical experience in studying failures in volumetric hydraulic drives *Hydraulics and Pneumatics Industrial* № 4(50) pp 3–14 http://pgpjournal.vsau.org/files/pdfa/2924.pdf
[8] Bergada J M, Kumar S and Watton J Axial 2012 Piston pumps, new trends and development *In book: Fluid Dynamics, Mechanical Applications and Role in Engineering* Chapter 1: Axial Piston Pumps, New trends and development pp 1–157 https://www.researchgate.net/publication/317178504_ Axial_Piston_Pumps_New_Trends_and Developmentcitation/download
[9] Qun Chao, Junhui Zhang, Bing Xu, Yuan Chen, and Yaozheng Ge 2012 Spline design for the cylinder block within a high-speed electro-hydrostatic actuator pump of aircraft *Meccanica* **1–2** pp 395–411 https://link.springer.com/article/10.1007/s11012-017-0705-2
[10] Larchikov I, Yurov A, Stazhkov S, Grigorieva A and Protsuk A 2014 Analysis of an Axial Piston Hydraulic Machine of Power Intensive Hydraulic Drive System. *Procedia Engineering* **69** pp 512–517 https://doi.org/10.1016/j.proeng.2014.03.020

[11] Shu Wang 2014 Robust Design of Piston Assemblies in an Axial Piston Pump *International Journal of Fluid Power* Vol 15 **2** pp 69–76 https://www.tandfonline.com/doi/abs/10.1080/14399776.2014.931131
[12] Zloto T and Stryjewski P 2017 Modeling the load of the kinematic pair piston-cylinder in an axial piston pump by means of FEA *Procedia Engineering* **177** pp 233–240 https://www.sciencedirect.com/science/article/pii/S1877705817307002
[13] Semenov S and Kulakov D 2019 Mathematical modeling of the mechanisms of volumetric hydraulic machines *IOP Conf. Series: Materials Science and Engineering* Vol 492 **1** p 16 https://iopscience.iop.org/article/10.1088/1757-899X/492/1/012042/pdf
[14] Shin Jung-Hun; Kim Hyoung-Eui and Kim Kyung-Woong 2011 A Study on Models for the Analysis of Pressure Pulsation in a Swash-Plate Type Axial Piston Pump *Tribology and Lubricants* Vol 27 **6** pp 314–320 http://www.koreascience.or.kr/article/JAKO201112961955353.page
[15] Helbig A and Boes C 2016 Electric Hydrostatic Actuation - modular building blocks for industrial applications *10th International Fluid Power Conference* Group 2 Novel System Structures pp 93–102.
[16] http://tud.qucosa.de/api/qucosa%3A29344/attachment/ATT-0/
[17] Stosiak M 2012 The modelling of hydraulic distributor slide–sleeve interaction *Archives of Civil and Mechanical Engineering* Vol 12 **2** pp 192–197 https://www.sciencedirect.com/science/article/abs/pii/S1644966512000313
[18] Wang H and Meng F L 2011 Simulation and Optimal Design of Cylinder Block of Axial Piston Pump Based on ANSYS J. *Advan. Mat. Res.* **186** pp 368–372 https://doi.org/10.4028/www.scientific.net/AMR.186.368
[19] Zheglova V, Khomiak Yu, Medvedev S and Nikolenko I 2017 Numerical and analytical evaluation of service life of the details axial piston hydraulic machines with complicated configuration under cyclic loading *Procedia Engineering* **176** pp 557–566 http://www.sciencedirect.com/science/journal/18777058/176
[20] Kutuzov V K, Voronov S A, and Sergeev Y V 2015 Research of influence of modes loading of axial-piston hydromachines on duration of their tests *Assembling in Mechanical Engineering and Instrument-Making* **95(6)** pp 38–41 https://www.mashin.ru/files/sbor6_08.pdf
[21] Hao M.and Qi X Y 2012 Modeling Analysis and Simulation of Hydraulic Axial Piston Pump *Advanced Materials Research* **430–432** pp 1532–1535 https://www.scientific.net/AMR.430-432.1532
[22] Zhang C, Wang S, Tomovic M And Hanc L 2017 Performance Degradation Analysis of Aviation Hydraulic Piston Pump Based on Mixed Wear Theory *Tribology in Industry* Vol 39 **2** pp 248–254 http://oaji.net/articles/2017/664-1514449256.pdf
[23] Quan Ling-Xiao, Cao Yua, Luo Hong-liang, Guo Rui and Guo Haixin 2015 Fatigue Analysis of the Cylinder in The Axial Piston Pump *Conference: Fluid Power and Mechatronics (FPM)* p 7 https://ieeexplore.ieee.org/document/7337096
[24] Ustinov A I, Falchenko Yu V, Melnichenko T V, Petrushinets L V, Lyapina K V, Shishkin A E and Gurienko V P 2015 Diffusion welding of steel to tin bronze through porous interlayers of nickel and copper *Paton Welding Journal* **9** pp 13–19 https://patonpublishinghouse.com/print/rus/journals/tpwj/2015/09/02
[25] Dashchenko A F and Nikolenko V I 2005 Calculation of the nominal pressure of axial-piston hydraulic machines by the geometric parameters of pumping units with hydraulic unloading *Transactions of Odessa Polytechnic University* **2(24)** pp 46–52 http://pratsi.opu.ua/app/webroot/articles/1312808449.pdf
[26] Borisov S P 2014 Prediction of the influence of structural factors on the fatigue resistance of materials *Scientific Bulletin of MSTU GA* **205** pp 67–73 https://avia.mstuca.ru/jour/article/view/630?locale=ru_RU

[27] Gutyrya S S, Medvedev S A, Khomyak Yu M and Chanchin A N 2017 Probabilistic analysis of fatigue durability of an epicycle of a wheel gearbox of the trolleybus *Bulletin of NTU "KhPI". Series: Problems of a mechanical drive* **25 (1247)** pp 37–43 http://dspace.opu.ua/jspui/handle/123456789/5764
[28] Troshchenko V T 2010 Fatigue of metals under nonuniform stressed state. Part 2. Methods of the analysis of research results *Strength of materials* Vol 42 **3** pp 241–257. https://link.springer.com/article/10.1007/s11223-010-9213-5